

WILTON MATERIALS RESEARCH CENTRE
MATERIALS SCIENCE GROUP

RHEOLOGY OF THERMOPLASTIC-CARBON FIBRE COMPOSITE IN THE ELASTIC AND
VISCOELASTIC STATES

INTRODUCTION

D J Groves/D M Stocks

The introduction of thermoplastic matrices to the field of continuous fibre reinforced composite materials brings new concepts of rapid composite fabrication. Unlike composites based on thermosetting resins where the matrix is chemically cured to form a cross-linked structure, the thermoplastic composite allows thermoforming of laminate structures. Cogswell (1) has reviewed the forming of laminates and subsequent shaping processes, which are performed essentially in the molten state. There will be a consequential re-organisation of fibre orientation, which will initially be chosen according to the performance requirements of an application. Such forming processes can be compared to metal forming technology (2), and some problems of forming complex curvatures have been described by Mallon et al (3).

In the shaping of a flat laminate, the deformation will be essentially in shear, either as intraply shear or interply slip. Characterisation of the shear rheology of thermoplastic composite has been reported using parallel plate rotational rheology (4). Small strain dynamic viscoelastic measurement was used to avoid displacement of the initial fibre orientations and interpretation by apparent Maxwell viscosity as a function of maximum shear rate was demonstrated for 60% carbon fibre and 60% glass fibre in polyether-etherketone. Both of these composites have a non-linear viscoelastic response and show an apparent yield stress of about 1KPa. This result was similar for laminate prepared from 0.125mm prepreg tapes compressed in the rheometer and pre-compressed plaques of the same dimensions. A change in matrix resin viscosity alters the higher stress viscosity but not the apparent yield stress (5).

Similar data with all fibres parallel or with alternate layers oriented at 0° and 90° in the platen plane, imply a nominally isotropic measurement. The shear strain is applied at all angles with respect to fibres. Along the fibre and transverse directions of viscosity have been obtained (6) using pairs of samples displaced symmetrically from the axis of oscillation in a similar dynamic viscoelastic measurement. Theory to resolve the along fibre and transverse dynamic moduli from oscillation of off-axis specimens has been derived by Rogers (7). The along fibre component of Maxwell viscosity shows the lower yield stress and correlates with the isotropic response, suggesting that the weaker direction may dominate the isotropic deformation and flow response (8). A uniform temperature over a large area of thermoplastic composite may be difficult to achieve during a shaping or forming process. Change in composite rheology with temperature is an unknown complication which may influence either or both of the uniformity of deformation and the level of retained stress.

The temperature dependence of the viscous and elastic responses are considered here, for a thermoplastic composite with about 60% carbon fibre in an amorphous polyaromatic matrix. This allows a transition from an elastic to viscous dominated response of the matrix polymer without problems of crystallisation.

The balance of the along fibre and transverse anisotropic response is investigated over the elastic to viscous transition in relation to the isotropic and matrix characteristics. The yield condition and interpretation, particularly relating dynamic and steady shear rheology have limitations.

EXPERIMENTAL

All measurements were made using a Rheometrics Mechanical Spectrometer over a range of temperatures between 240° and 340°. Parallel disc platens were used with rotation or oscillation about the cylindrical axis to accommodate the planar laminated ply specimens. Steady shear flow in the plane of lamination will change the initial fibre orientation, introducing a level of uncertainty defining the orientation after measurement. Different shear rates require different times and different total shear strains for the flow to achieve equilibrium. The main characterisation was therefore performed by small strain oscillation to obtain complex modulus and phase angle leading to the dynamic viscosity and modulus. The system for isotropic measurements is shown in Fig 1. Platen diameters of 10mm and 25mm were used.

A symmetrical pair of off-centre specimens were used for resolving the along fibre and transverse data and located in position using a template as shown in Fig 2. A single off-centre specimen had a tendency to move as previously described (6). Specimens were normally 15mm square with centres separated by 25mm using 50mm diameter platens. However, at lower temperatures of 280°C or less, to compensate for increasing torque, specimens were 10mm square with centres separated by 15mm. The direction of fibre orientation was the same for both off-centre specimens in each measurement because the phase angle was found to vary with the angle of orientation. In the case of mixed orientation, the mean phase angle which is determined may reduce the accuracy of subsequent analyses.

SAMPLE PREPARATION

All samples were made by high pressure lamination of 12 ply layers of prepreg. All fibres were parallel. The material was machined to squares of the required size (10mm, 15mm or 25mm) and then reduced to the octagonal shape in Fig 1 for the isotropic measurements.

Pairs of specimens for the along fibre and transverse measurements were carefully chosen to be as close to the same thickness as possible. An initial thickness of 2.0mm was squeezed to 1.8mm when melted between the rheometer platens. Squeezing of different thicknesses may result in preferential loss of matrix polymer and a consequential change in volume fraction, and therefore a slightly different material.

MEASUREMENTS

The rheometer temperature is measured at the centre of the lower hastalloy disc platen. As the matrix polymer melts through the composite thickness between the platens, the initial normal loading of up to 1kg relaxes. Five minutes after reaching the set temperature was sufficient for a uniform temperature to develop and stress relaxation to be completed. The hot gas oven used an inert nitrogen atmosphere to ensure polymer stability for the duration of the measurement.

(a) Dynamic Measurement

The torque and strain amplitude vectors were used to calculate the complex modulus (G^*) from the maximum shear stress and shear strain. The phase angle (δ) further allows the in-phase storage modulus (G') and the quadrature loss modulus (G'') to be measured assuming linear viscoelasticity with a sinusoidal response for an isotropic sample. The moduli G' and G'' were measured as functions of angular frequency (ω) for the isotropic case to express dynamic viscoelastic response and of strain amplitude to establish the limits of linearity. Complex viscosity, $\eta^* = G^*/\omega$, and dynamic viscosity, $\eta' = \eta^* \sin\delta$, were calculated following the same criteria for linearity.

For the anisotropic response along and normal to the fibres, the torque and phase angle were measured as a function of strain amplitude. This provides the data in a convenient form for the theory (7) and simultaneously demonstrates the linearity of the strain response.

Input and output sinusoidal waveforms were monitored by an oscilloscope with a digital storage adaptor throughout all of the measurements. Only data from visually good waveforms has been used in the analysis. Previous use of a frequency spectrum analyser (4) has demonstrated that a visually good waveform, together with the same value for input command strain and measured strain, is usually free from harmonic problems. Each data set is the mean of three measurements.

(b) Steady Shear Measurements

Equilibrium torque for the shear stress is measured as a function of steady shear rate in both clockwise and counter clockwise directions, which tends to maintain the fibre orientation at low shear rates. However, as the shear rate increases, so the total strain to achieve an equilibrium torque increases with risk of fibre displacement, so shear rate was limited to 0.5 sec^{-1} .

RESULTS AND DISCUSSIONS

The thermal stability of the composite was first checked by monitoring the dynamic moduli for 45 minutes. A drop in values of about 5% was noted, but the changes over shorter times were not significant in terms of frequency or strain sweep errors.

(a) Isotropic

The aromatic matrix polymer has an apparent complex viscosity of 8×10^6 Pas at 0.1 rad/sec at 240°C falling to 1.2×10^3 Pas at 340°C. The polymer is rubbery at 240°C and a viscous fluid which is only slightly shear thinning at 340°C. A plot of phase angle, $\tan\delta$, as a logarithmic function of temperature in Fig 3, shows an almost linear relationship with $\tan\delta = 1$ in the temperature range 250°C at 1rad/sec to 270°C at 10rad/sec. We can therefore define the frequency dependent rubber to fluid transition as being in this temperature range. This defines a relationship of the form:-

$$\tan\delta = Ae^{BT}$$

through the transition zone. Approximate values of $A = 5.5 \times 10^{-9}$ and $B = 3.5 \times 10^{-2}$. In the fluid state the matrix response is linear viscoelastic.

The composite has a non-linear viscoelastic response at all temperatures, and different strain amplitudes result in different frequency dependences for the dynamic viscosity and dynamic modulus as in Fig 4 for 340°C. While in the viscous fluid or melt state, the treatment as a Maxwell fluid, following Benbow Cogswell and Cross(8) reduces the level of strain dependence as found for other composites (4,5,6,8). Apparent Maxwell viscosity at 290°C and 340°C

$$\eta_M = \eta' / \sin^2\delta$$

versus maximum shear rate $\dot{\gamma} = \omega\gamma_0$ is given in Fig 5.

(η is dynamic viscosity, ω is angular frequency and γ_0 is maximum strain). Limited range steady shear viscosity is included for comparison. When the Maxwell viscosity is taken as a function of shear stress, an approximate yield stress is identifiable from the stress asymptote. The apparent yield stress is temperature dependant, rising more rapidly in the rubbery state, as shown by the stress at a viscosity of 10^7 Pas and 1% strain in Fig 6.

The Maxwell viscosity does not converge the strain dependence of the viscoelasticity in the elastic region at 240°C or 250°C. The equivalent Maxwell modulus $G_M = 1/\cos^2\delta$ does not converge the strain dependence for any temperature either in the elastic or fluid states.

(d) Along Fibre and Transverse

The in-phase and quadrature moduli G' and G'' in the along fibre and transverse directions were determined from torque measurements at 1, 2, 5 and 8% strain for angular frequencies up to 10rad/sec. At the lower temperatures only a limited range of conditions were used due to restrictions imposed by increased torque, particularly in the rubbery state. Dynamic viscosity and elasticity along the fibres and in the transverse direction were determined using off-centre oscillation analysis(7), then converted to the apparent Maxwell parameters.

The Maxwell viscosity is plotted as a function of shear rate in Fig 7 and shear stress in Fig 8. The lowest shear stress data points in the two directions were determined at 0.1 rad/sec and are subject to a longer residence time. A small upward correction is therefore needed. We speculate that approximate yield stresses are 10^3 Pa or less along the fibres and about 2×10^3 Pa in the transverse direction at 340°C .

At lower temperatures it was only possible to obtain data at low frequencies or low strains to avoid slip or harmonic waveforms. The dependence of the Maxwell viscosity or temperature is shown in Fig 9 for along fibre and Fig 10 for transverse, as a function of shear stress, using data from 1rad/sec. The tendency for a lower yield stress in the along fibre directions is evident at temperatures down to about 280°C . As the rubbery state is approached, the yield stresses in the two direction tend to coincide. Again the strain dependence does not converge in the rubbery state.

The equivalent Maxwell modulus measured at 1rad/sec has a temperature dependence as shown in Fig 11 for along the fibre and Fig 12 for the transverse direction. Expressed as a function of shear stress, G_M covers two decades for the along fibre direction but only one and a half decades for the transverse direction and is more sensitive to fibre direction than η_M . However, the strain dependence of G_M does not converge as shown for the single temperature of 340°C , along the fibre in Fig 13 and transverse in Fig 14. The strain and angular frequency axes of the grid are indicated. It is seen that the frequency dependence at 340°C is slightly less in the along fibre than in the transverse direction, showing the opposite pattern to temperature dependence. There appears to be some similarity to solid elasticity, but a detailed comparison for this material has not been possible.

CONCLUSIONS

An amorphous thermoplastic structural composite has a non-linear viscoelastic response as determined from small strain oscillatory shear, whilst its matrix resin has a linear viscoelastic response and a power law relationship between $\tan\delta$ and temperature which is continuous through the rubber to fluid transition.

The concept of an apparent Maxwell viscosity and maximum shear rate provides an interpretation of dynamic viscosity which is independent of strain amplitude in the fluid melt state but not in the rubbery state. Similar rules apply to Maxwell viscosity components in the along and transverse fibre directions determined from off-axis oscillation.

Apparent yield stresses are temperature dependent with a sharper rise with decreasing temperature in the rubbery state. Yield stress is lower along the fibres than in the transverse direction. The magnitude of 1KPa is consistent with values for the thermoplastic composites having around 0.6 volume fraction of fibres, emphasising the role of the fibre packing.

The apparent Maxwell modulus interpretation of dynamic modulus is strain amplitude dependent in all of the conditions examined. The temperature dependence has a greater sensitivity in the transverse direction. The frequency and strain dependence appear to be coupled, although further studies may be need to establish a full frequency-strain-temperature relationship.

REFERENCES

- 1 F N Cogswell 'The Processing Science of Thermoplastic Structural Composites' Int. Polym. Process 1 No. 4 (1987) p157.
- 2 J B Cattanch, F N Cogswell, in: Developments in Reinforced Plastics 5, Ed. G Pritchard (Elsevier 1986).
- 3 P J Mallon, C M O'Brádaigh, R B Pipes 'Polymeric Diaphragm Forming of Complex-Curvature Thermoplastic Composite Parts' Composites 20 No 1 (1989) p48.
- 4 D J Groves 'A Characterisation of Shear Flow in Continuous Fibre Thermoplastic Laminates' Composites 20 No 1 (1989) p28.
- 5 F N Cogswell, D J Groves, 'The Melt Rheology of Continuous Fibre Reinforced Structural Composite Materials', Proc. Xth Internat. Congr. Rheol (1988) Sydney Aug 14-19.
- 6 D J Groves, A M Bellamy, D M Stocks, 'Isotropic and Anisotropic Shear Flow in Continuous Fibre Thermoplastic Composites' Proc 3rd European Rheology Conf. (1990) Edinburgh Sept 3-7.
- 7 T G Rogers 'Rheological Characteristics of Anisotropic Materials' Composites 20 No 1 (1989) p21.
- 8 D J Groves, A M Bellamy, D M Stocks, 'Anisotropic Rheology of Continuous Fibre Thermoplastic Composites'. To be published.
- 9 J J Benbow, F N Cogswell, M M Cross, 'On the Dynamic Response of Viscoelastic Fluids'. Rheol. Acta 15 (1976) p231.

Fig 1 PLATEN GEOMETRY FOR ISOTROPIC MEASUREMENTS

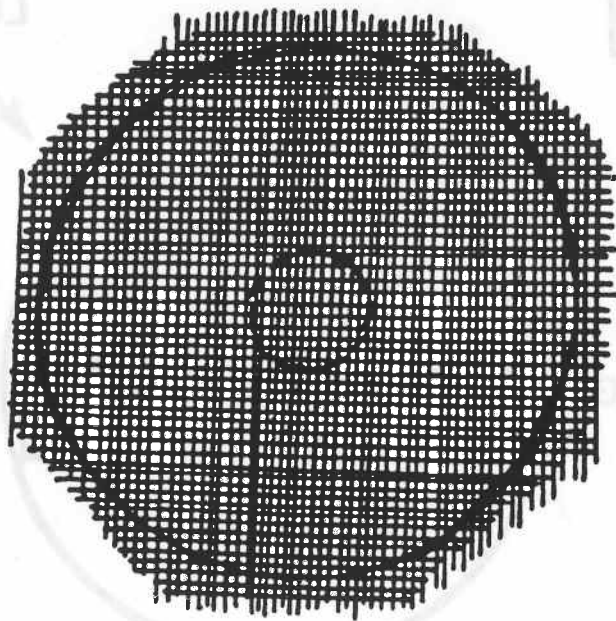
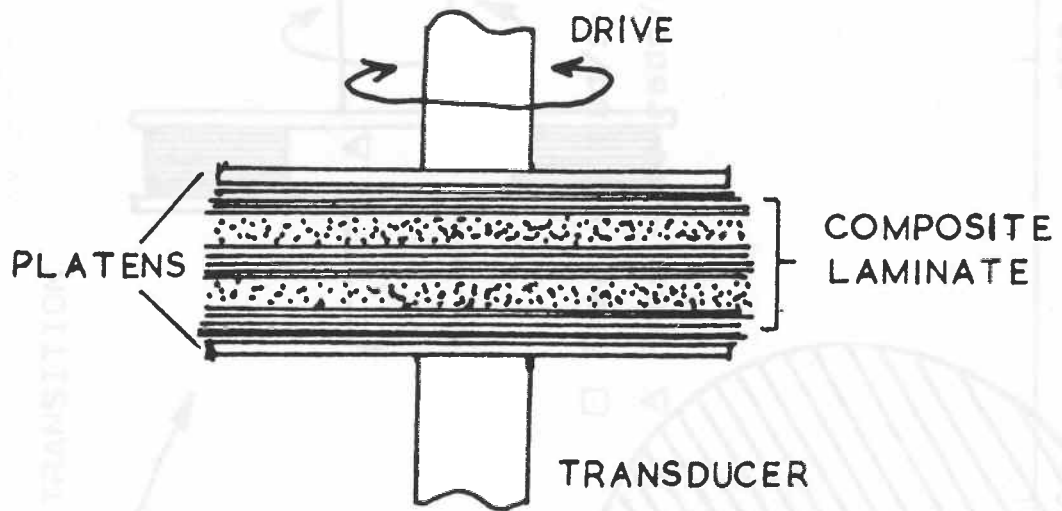


Fig.2 OFF AXIS GEOMETRY FOR ANISOTROPIC MEASUREMENTS

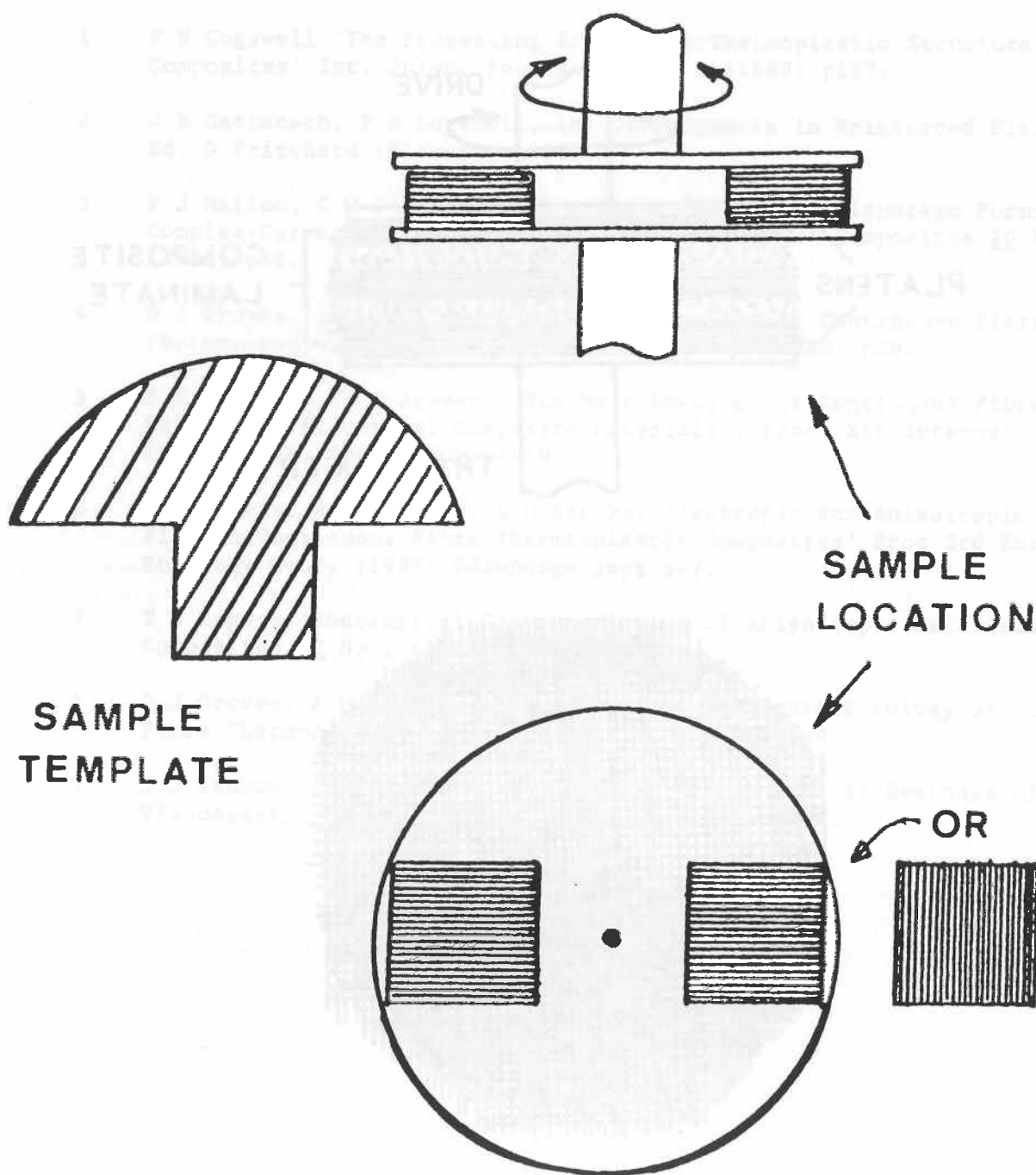


Fig 3 TEMPERATURE DEPENDENCE OF PHASE ANGLE.

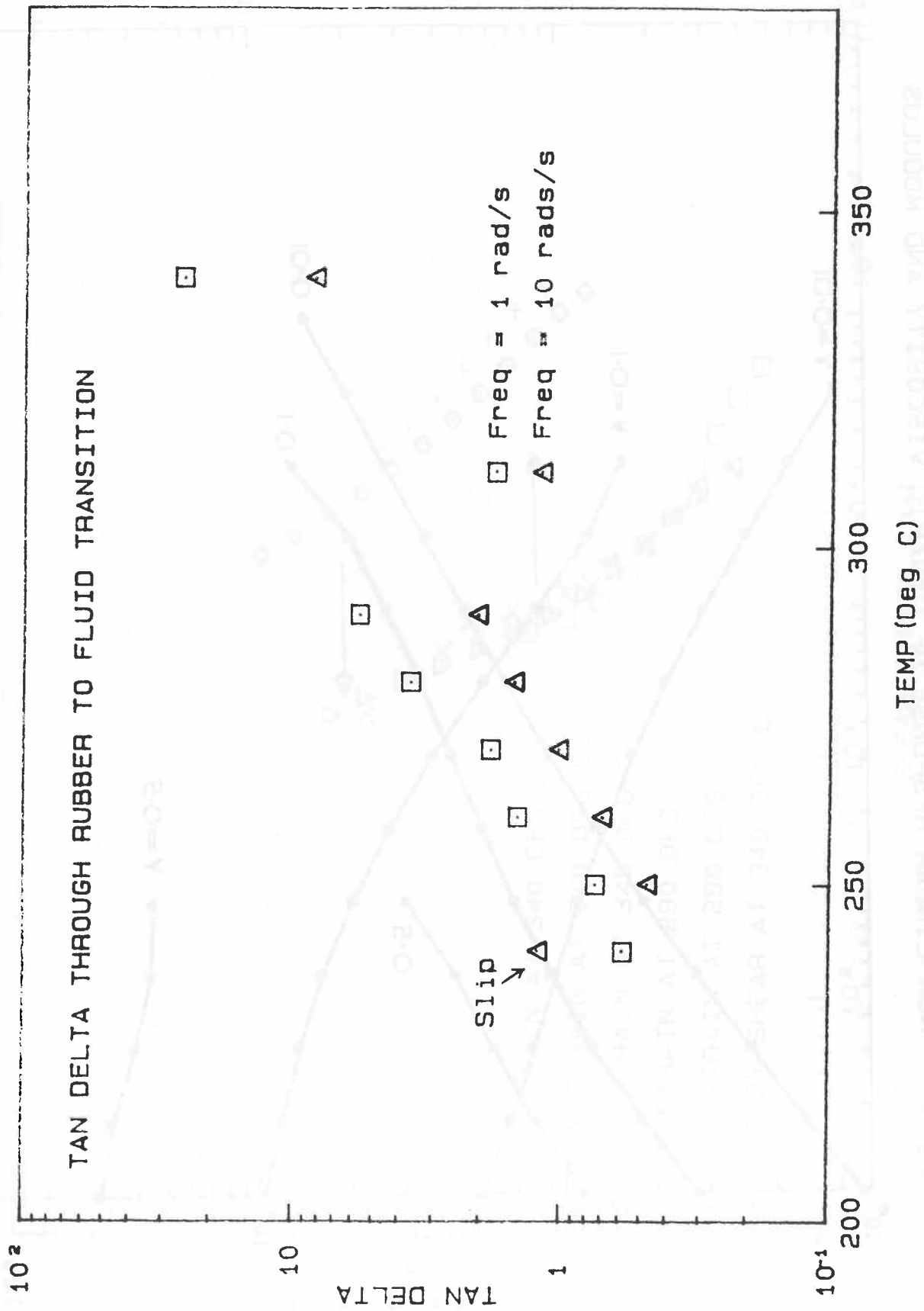


Fig 5 APPARENT MAXWELL VISCOSITY AND STEADY SHEAR VISCOSITY.

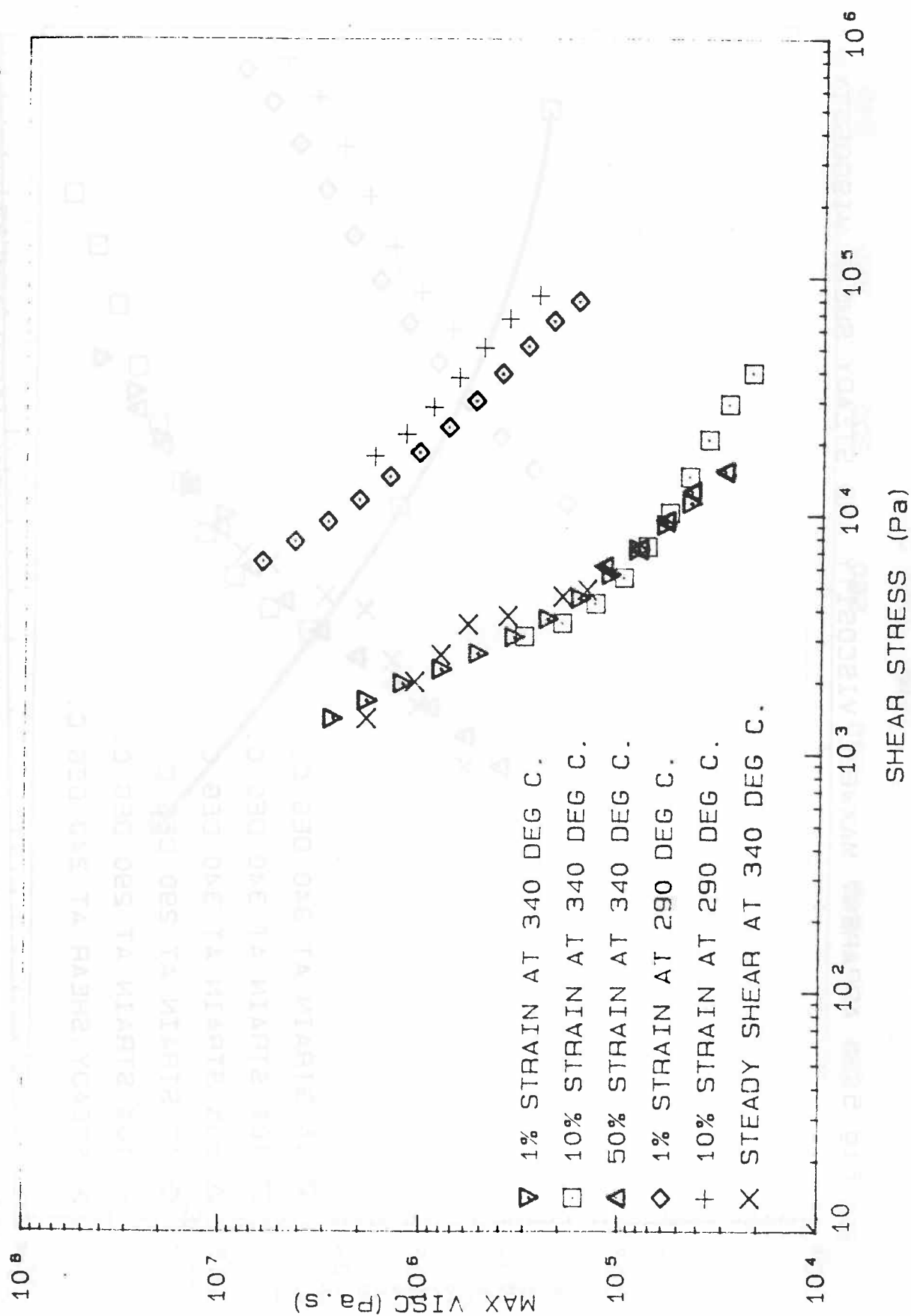


Fig 5 APPARENT MAXWELL VISCOSITY AND STEADY SHEAR VISCOSITY.

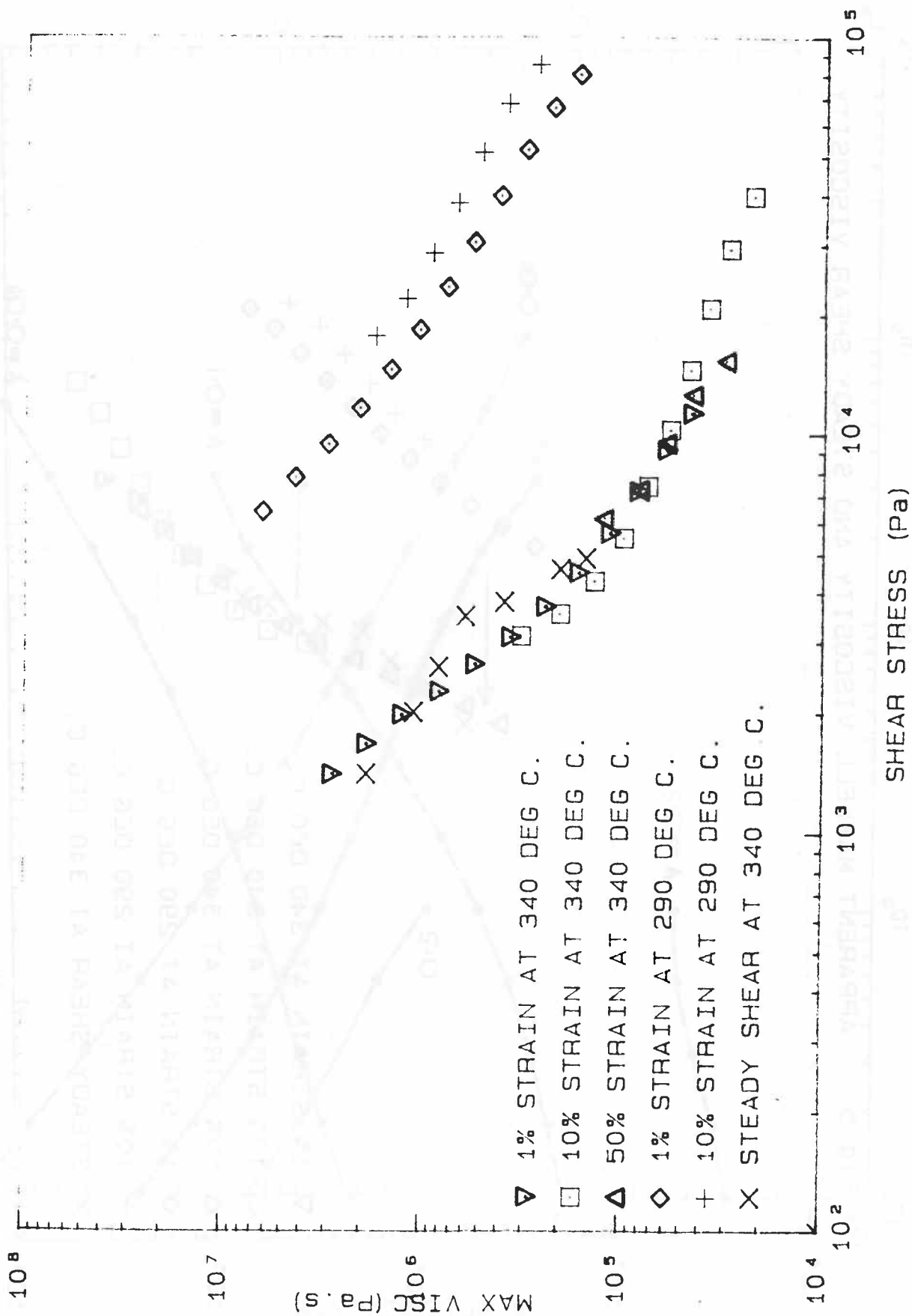


Fig. 6 TEMPERATURE DEPENDENCE OF APPARENT YIELD STRESS

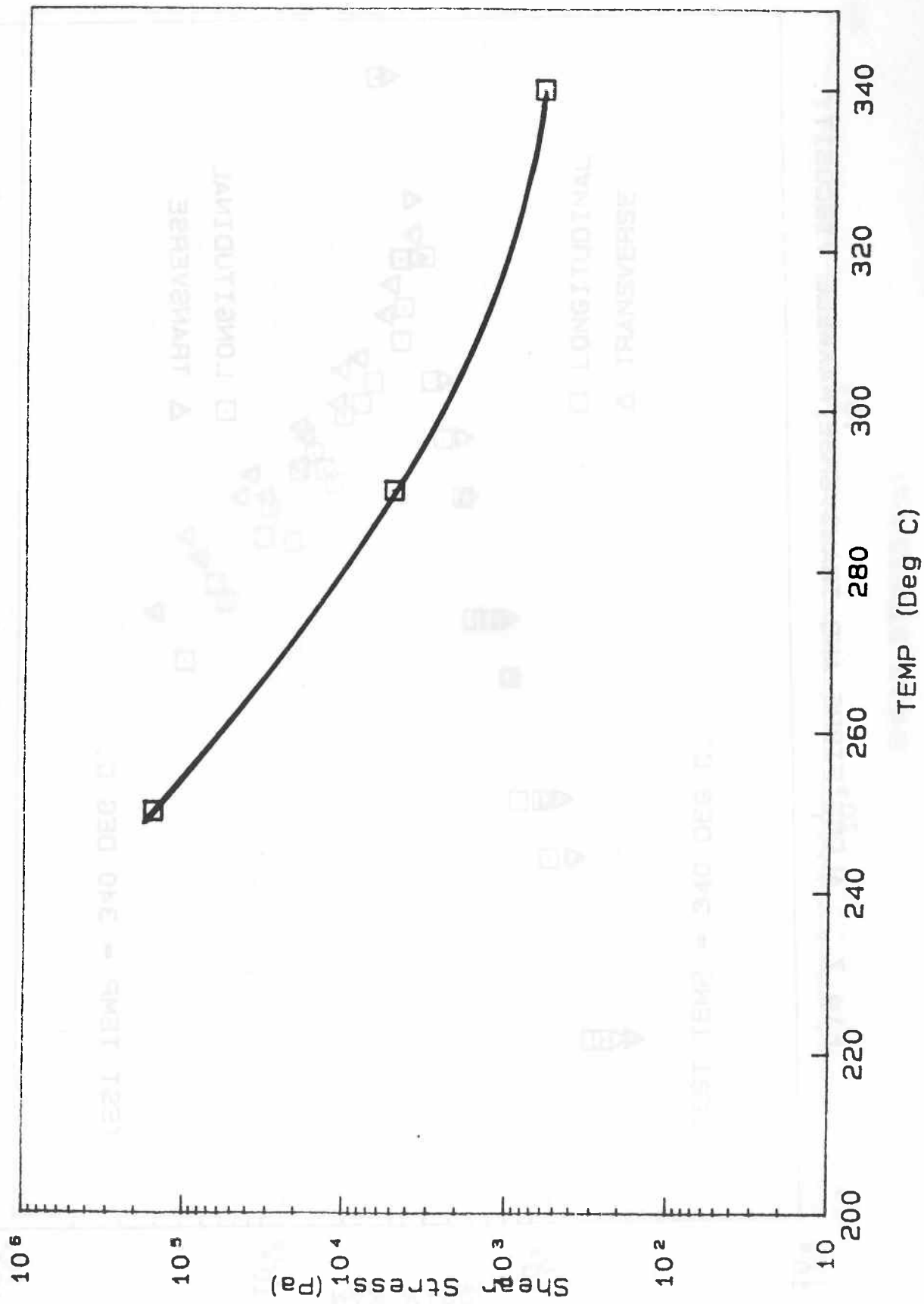


Fig 7 ALONG FIBRE AND TRANSVERSE MAXWELL VISCOSITY.

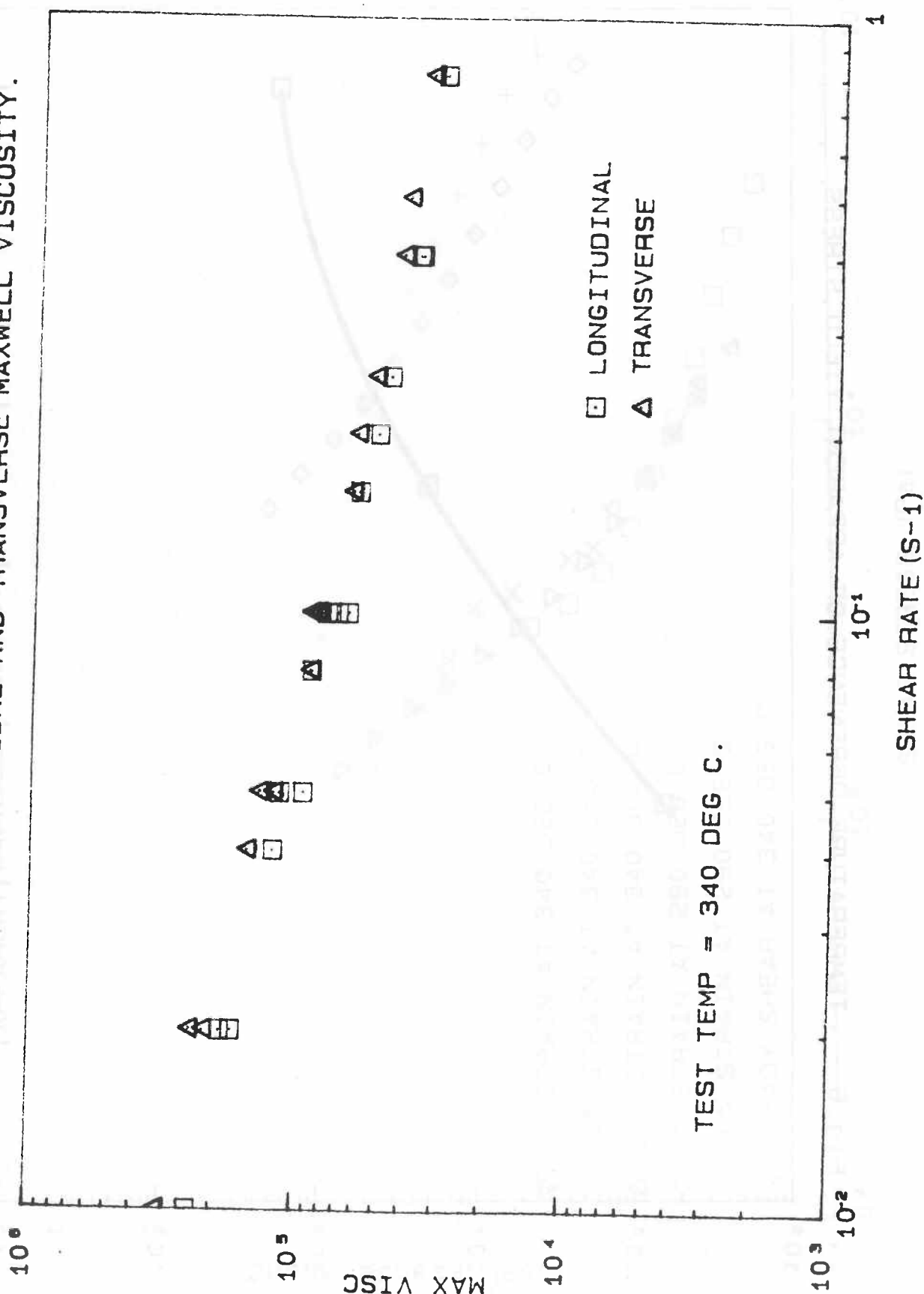


Fig 8 ALONG FIBRE AND TRANSVERSE MAXWELL VISCOSITY.

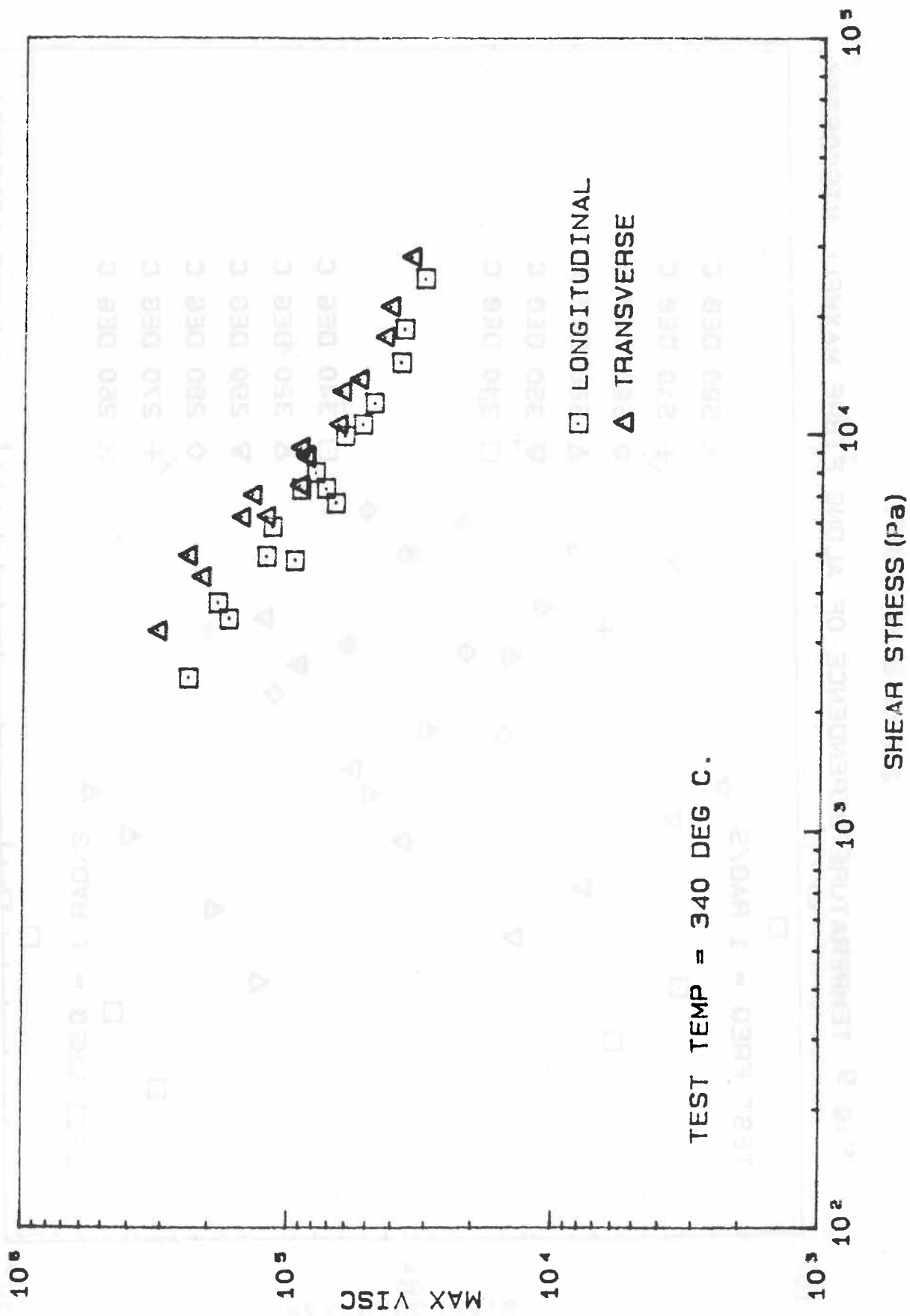


Fig 9 TEMPERATURE DEPENDENCE OF ALONG FIBRE MAXWELL VISCOSITY.

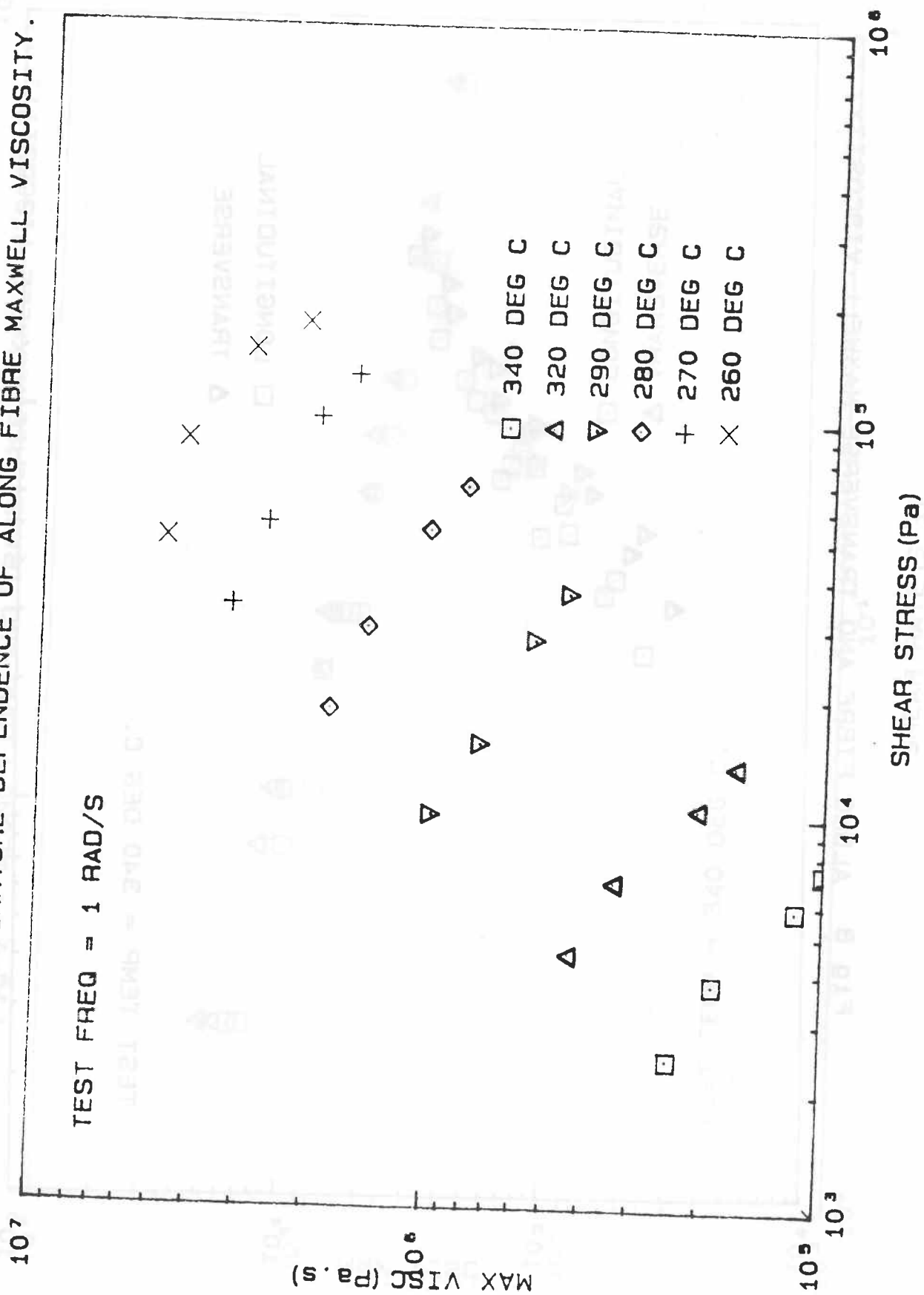


Fig 10 TEMPERATURE DEPENDENCE OF TRANSVERSE MAXWELL VISCOSITY.

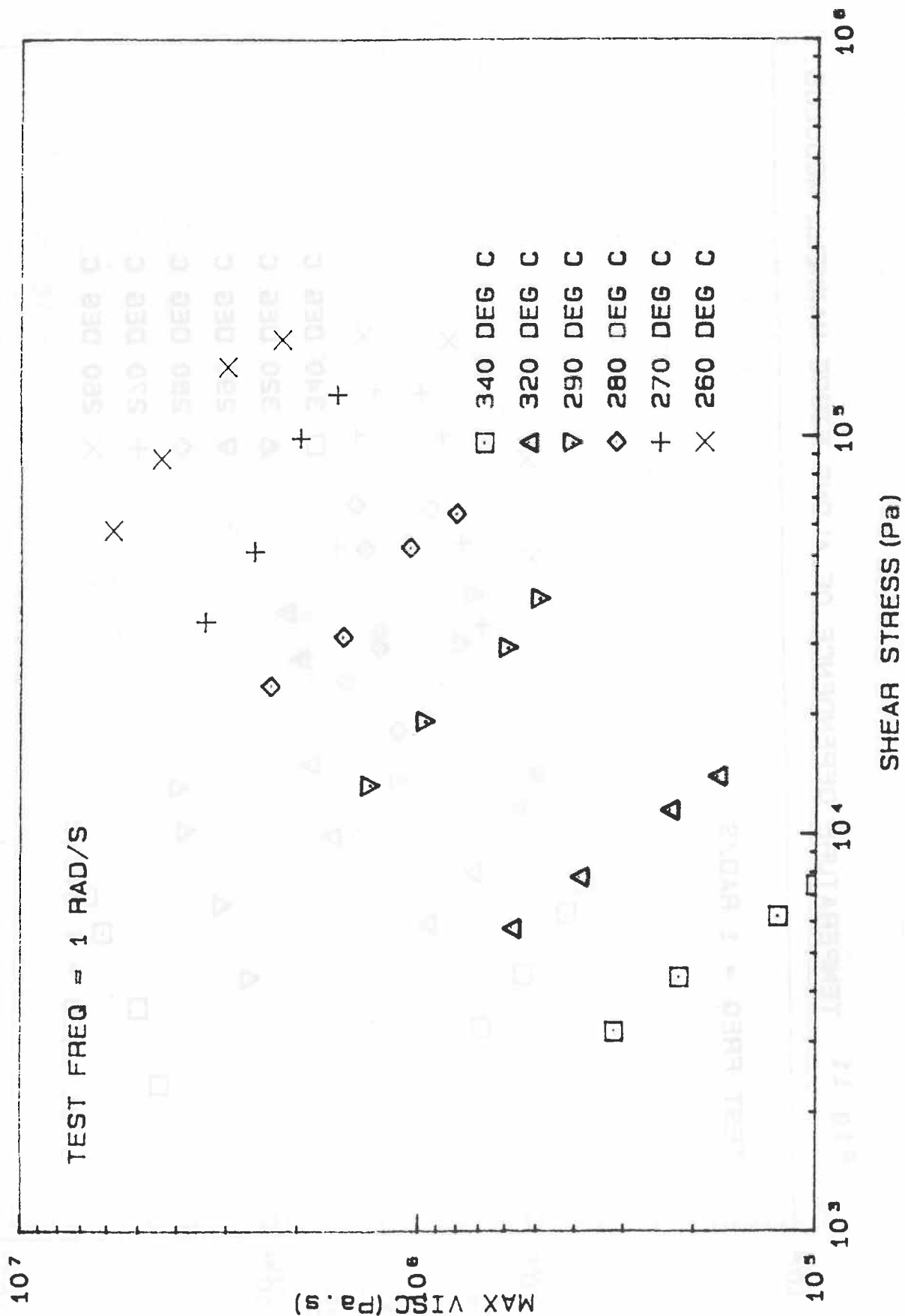


Fig 11 TEMPERATURE DEPENDENCE OF ALONG FIBRE MAXWELL MODULUS.

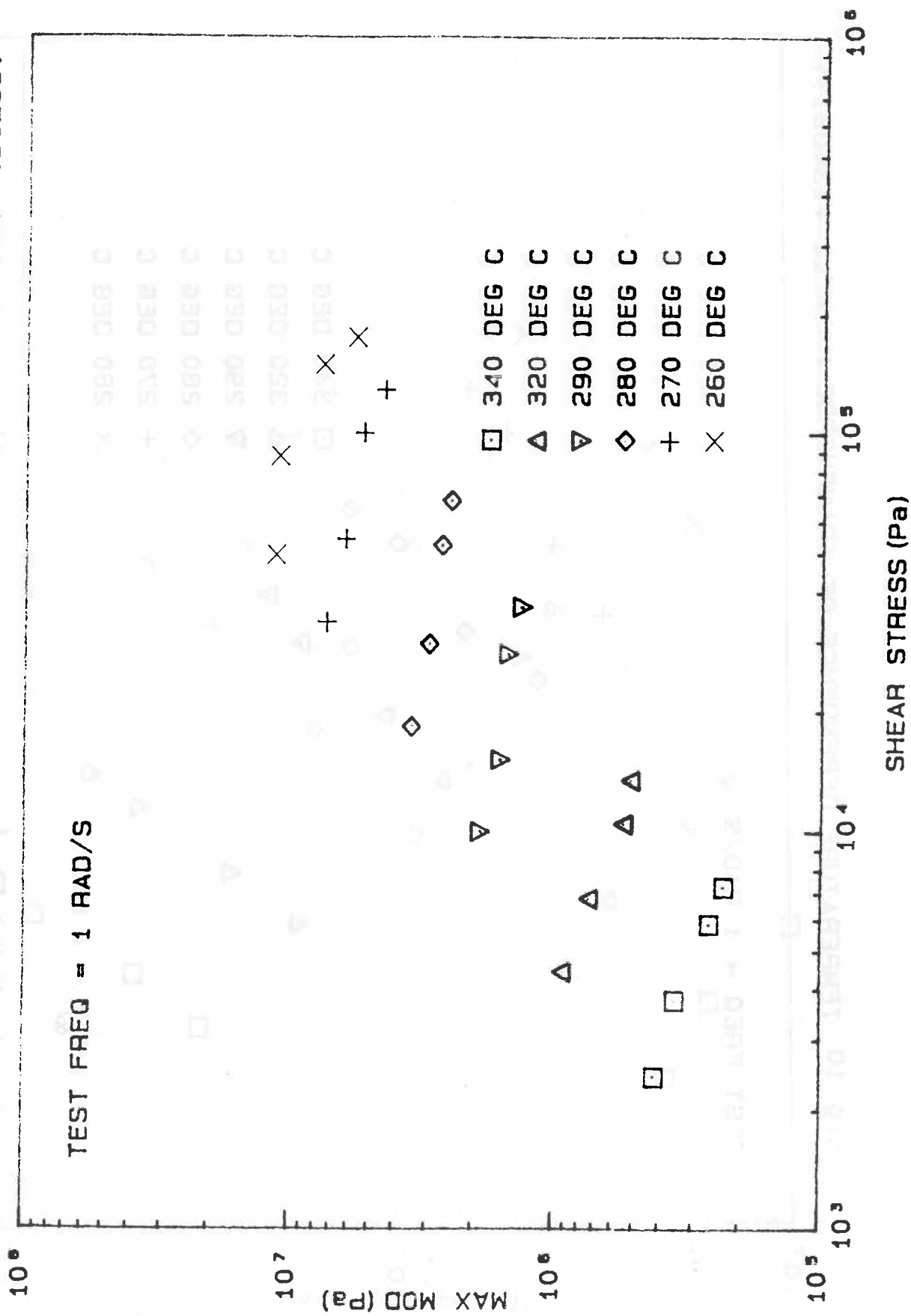


Fig 12 TEMPERATURE DEPENDENCE OF TRANSVERSE MAXWELL MODULUS.

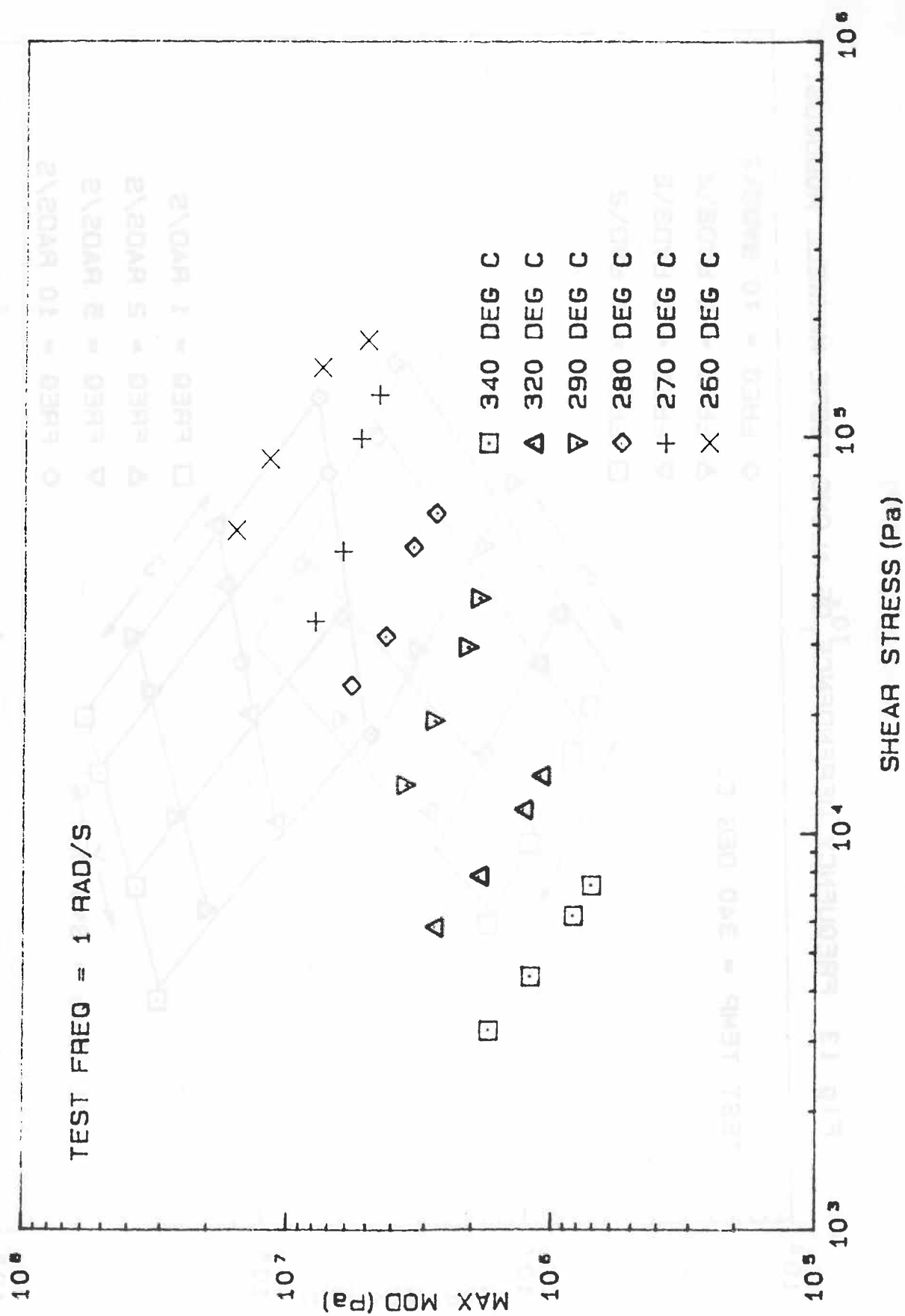


Fig 13 FREQUENCY DEPENDENCE OF ALONG FIBRE MAXWELL MODULUS.

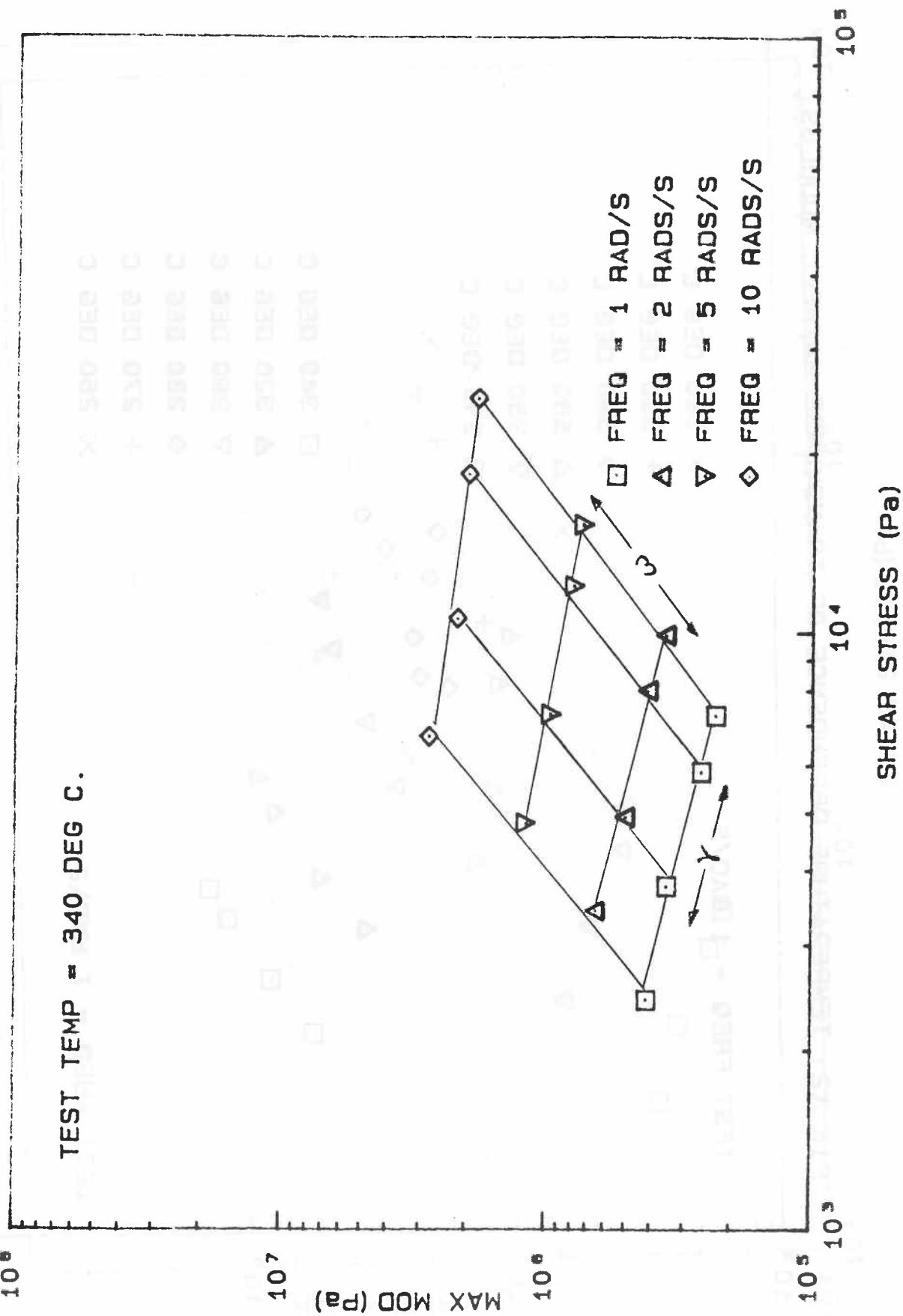


Fig 14 FREQUENCY DEPENDENCE OF TRANSVERSE MAXWELL MODULUS.

